

Unprecedented Inversion of Configuration at Carbon in the Electrophilic Cleavage of the Carbon–Zirconium(IV) Bond

Maria Zablocka,[†] Alain Igau,[‡] Nathalie Cenac,[‡] Bruno Donnadiou,^{‡,||} Françoise Dahan,^{‡,||} Jean Pierre Majoral,^{*,‡} and Michal K. Pietrusiewicz^{*,†,§}

Contribution from the Centre of Molecular and Macromolecular Studies, Polish Academy of Sciences, Sienkiewicza 11290-362 Lodz, Poland, and Laboratoire de Chimie de Coordination du CNRS, 205, route de Narbonne, 31077 Toulouse Cédex, France

Received January 3, 1995[®]

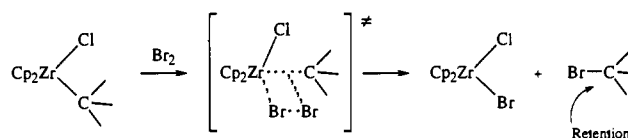
Abstract: Exchange reactions between the α -zirconated phospholane **3**, obtained by the addition of $[\text{Cp}_2\text{ZrHCl}]_n$ (**2**) to the dihydrophosphole **1**, and dimethyl- or diphenylchlorophosphine **4a** or **4b** or bis(diisopropylamino)- or -bis(dicyclohexylamino)phosphenium salts **5a** or **5b**, proceed with inversion of configuration at the α -substituted phospholane carbon atom and lead to diphosphines **6a,b,d,e**. The optically active dihydrophosphole (R_P)-**1** reacts with $[\text{Cp}_2\text{ZrHCl}]_n$, then diphenylchlorophosphine to give the 1,1-diphosphine **6b*** isolated in the form of the optically active diphosphine disulfide (R_P)-**14**, which is characterized by X-ray diffraction studies (crystal data for (R_P)-**14**: orthorhombic, $P2_12_1$, $a = 8.391(5)$ Å, $b = 10.880(3)$ Å, $c = 22.651(6)$ Å, $R = 0.038$). In contrast, retention of configuration at the α -substituted phospholane carbon atom in **3** is observed when **3** is reacted with the chlorodiazaphospholane **4c**, giving rise to the diphosphine **6c** isolated in the form of the diphosphine disulfide **15**. **15** is characterized by X-ray diffraction studies (crystal data for **15**: monoclinic, $P2_1/C$, $a = 8.243(5)$ Å, $b = 23.468(3)$ Å, $c = 9.412(6)$ Å, $R = 0.042$). Comparison of the structures of **3**, **6b**, (R_P)-**14**, and **15** is done on the basis of NMR data, molecular modeling, and X-ray crystallographic studies.

Introduction

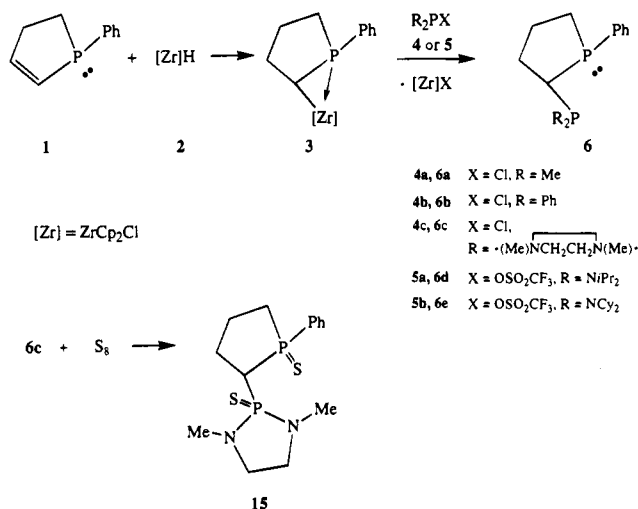
Mechanisms for electrophilic cleavage of the carbon–metal bond in transition metal alkyls can be elucidated with the observation of the stereochemical consequence, at carbon, of the cleavage process.^{1–3} Schwartz et al.⁴ have examined the stereochemistry at carbon in the electrophilic cleavage reactions involving bis(η^5 -cyclopentadienyl)(chloro)alkylzirconium(IV) complexes. The authors found that this reaction proceeded with retention at carbon; they proposed a transition state in which the electrophilic reagent was coordinated to zirconium by donation of a pair of electrons to its available vacant low-lying orbital, facilitating front-side attack on the C–Zr bond⁴ (Scheme 1).

We have previously reported⁵ that the hydrozirconation of dihydrophosphole **1** with $[\text{Cp}_2\text{ZrHCl}]_n$ (**2**) gave the α -zirconated phospholane **3**, which on subsequent treatment with chlorophosphines **4a,b** or phosphenium salts **5a,b** led diastereoselectively to new 1,1-diphosphines⁶ **6a,b,d,e** (Scheme 2), Cis

Scheme 1. Transition State for Electrophilic Cleavage of the C–Zr Bond



Scheme 2. Synthesis of Diphosphines **6** and Diphosphine Disulfide **15**



[†] Polish Academy of Sciences.

[‡] Laboratoire de Chimie de Coordination du CNRS.

[§] Present address: Department of Organic Chemistry, Maria Curie-Skłodowska University, ul. Gliniana 33, 20-031 Lublin, Poland.

^{||} X-ray analyses.

[®] Abstract published in *Advance ACS Abstracts*, July 15, 1995.

(1) Bock, P. L.; Boschetto, D. J.; Rasmussen, J. R.; Demers, J. P.; Whitesides, G. M. *J. Am. Chem. Soc.* **1974**, *96*, 2814 and references therein.

(2) Jensen, F. R.; Madan, V.; Buchanan, D. H. *J. Am. Chem. Soc.* **1971**, *93*, 5238.

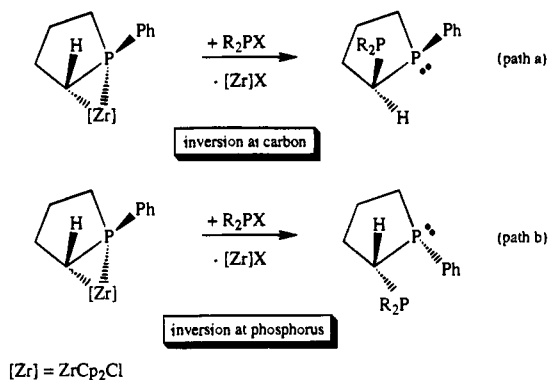
(3) (a) Anderson, S. M.; Ballard, D. H.; Chrastowski, J. Z.; Dodd, D.; Johnson, M. D. *J. Chem. Soc., Chem. Commun.* **1972**, 685. (b) Flood, T. C.; DiSanti, F. J. *J. Chem. Soc. Chem. Commun.* **1975**, 18.

(4) (a) Labinger, J. A.; Hart, D. W.; Siebber, W. E., III; Schwartz, J. J. *Am. Chem. Soc.* **1975**, *97*, 3851. (b) Carr, D. B.; Schwartz, J. *Ibid.* **1979**, *101*, 3521.

(5) Zablocka, M.; Boutonnet, F.; Igau, A.; Dahan, F.; Majoral, J. P.; Pietrusiewicz, K. M. *Angew. Chem., Int. Ed. Engl.* **1993**, *32*, 1735.

(6) C₂-Symmetric bis(phospholanes) and their use in enantioselective hydrogenation reactions have been reported by M. J. Burk. See, for example: Burk, M. J.; Feaster, J. E. *J. Am. Chem. Soc.* **1992**, *114*, 6266. Burk, M. J. *Ibid.* **1991**, *113*, 8518.

Scheme 3. Possible Stereochemical Pathway for C–Zr Electrophilic Cleavage Process in the Exchange Reaction of **3** with **4** or **5**



configuration at carbon of the C–Zr bond (Scheme 3, path a) or with pyramidal inversion at phosphorus (Scheme 3, path b),⁷ In order to distinguish between the two alternative pathways (Scheme 3), it was necessary to carry out the detailed studies of the structure and the configurational stability at phosphorus of the phospholanes **3** and **6**,

We now wish to disclose the results of these studies from which it follows that the electrophilic cleavage of the C–Zr bond of the α -zirconated phospholane **3** occurred with *inversion of configuration at carbon*,

Results and Discussion

The found unexpected stability of the α -zirconated phospholane **3** can be viewed as a consequence of the complexation of the zirconium moiety Cp₂ZrCl with the lone pair of the P-phospholane atom. Such a complexation induced a trans arrangement between the CH proton of the three-membered ring P–CH–Zr and the lone pair of phosphorus engaged in a dative bond with the low-lying vacant 1a₁ orbital of the zirconium metallocene (Figure 1).⁸

NMR spectroscopic data and chemical evidences have been found to prove such a trans arrangement in **3**. It has been already shown that ¹H NMR spectra of cyclic phosphines are useful in deducing stereostructures of such compounds and that ²J_{HP} can be used as one of the highly diagnostic parameters in this regard.^{9,10} For example, ²J_{HaP} and ²J_{HbP} for the dihydrophosphole shown in Figure 2 were found to be 6 and 25 Hz, respectively.¹⁰ Analogous observations were made for the corresponding oxides.¹¹ A ²J_{HP} of 4.1 Hz in **3** was observed for the proton bonded to the metallated carbon atoms of the phospholane ring and its value fitted well with the proposed trans configuration of **3**. Moreover, small coupling constants ³J_{HP} and ²J_{CP} (0.6 and 2.7 Hz, respectively), which could be considered typical for three-membered phosphametallacycles, were detected between the phosphorus atom and the protons and carbons of the Cp ligands. Indeed similar coupling constants were already observed in analogous three-membered

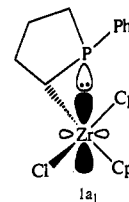


Figure 1.

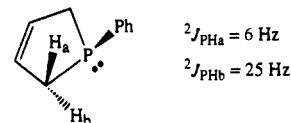
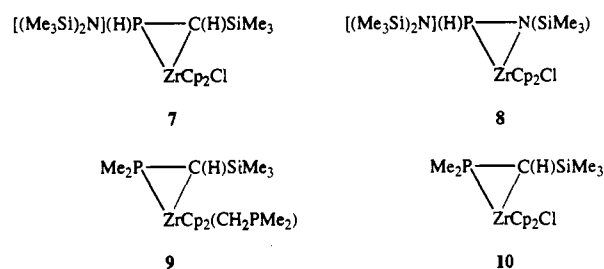


Figure 2.

phosphametallacycles such as **7** and **8**.¹² Furthermore, the large one-bond coupling constant ¹J_{CP} of 51.7 Hz in **3** was characteristic for P(IV)-phospholane structures.¹³ This value also compared well with the values reported for other three-membered rings like **9** (¹J_{CP} = 45.0 Hz)¹⁴ or **10** (¹J_{CP} = 46.0 Hz).¹⁵ Attempts to obtain X-ray quality crystals of the α -zir-



conated phospholane **3** failed. In order to have an insight of the structure of **3** we have investigated the molecular modeling (MM2 parameters, CAChe system). The lowest energies correspond to the two possible η^2 -bonding modes:¹⁶ “P-outside”, out-**3**, and “P-inside”, in-**3**, type structures (Figure 3). The Zr–P distances (d_{Zr-P} = 2.9 Å) found in out/in-**3** modeling structures were in accord with those observed in the literature (2.78 > d_{Zr-P} > 2.9 Å for three-membered ring P–CH–Zr^{14,15,17}),

The presence of a P–CH–Zr skeleton in compound **3** has been also chemically demonstrated. Electrophilic attack of BH₃ on the phosphorus atom of **3** induced the dissociation of the phosphorus–zirconium dative bond and as expected¹⁸ the migration of the ZrCp₂Cl moiety from the α to β position (Scheme 4).⁵ The observed migration corroborated further the importance of the phosphorus lone pair of electrons in the stabilization of the metal in the α position in **3**. The insertion reaction of :C=N–CH₂SiMe₃ into the C–Zr bond of **3** (Scheme 4) generated compound **11**. As expected for such compounds no coupling constants ³J_{HP} and ²J_{CP} were observed between the phosphorus atom and the protons and carbons of the Cp ligands,

(12) Dufour, N.; Caminade, A.-M.; Basso-Bert, M.; Igau, A.; Majoral, J. P. *Organometallics* **1992**, *11*, 1131–37.

(13) Gray, G. A.; Cremer, S. E.; Marsi, K. L. *J. Am. Chem. Soc.* **1976**, *98*, 2109.

(14) Karsch, H. H.; Grauvogel, G.; Deubelly, B.; Müller, G. *Organometallics* **1992**, *11*, 4238.

(15) Karsch, H. H.; Grauvogel, G.; Kaweck, M.; Bissinger, P. *Organometallics* **1993**, *12*, 2757.

(16) For η^2 -iminoacyl chemistry, see for example: Erker, G.; Mena, M.; Krüger, C.; Noe, R. *Organometallics* **1991**, *10*, 1201. Durfee, L. D.; Rithwell, I. P. *Chem. Rev.* **1988**, *88*, 1059–79.

(17) Karsch, H. H.; Grauvogel, G.; Kaweck, M.; Bissinger, P.; Kumberger, O.; Schier, A.; Müller, G. *Organometallics* **1994**, *13*, 610.

(18) Labinger, J. A. In *Comprehensive Organic Synthesis*; Trost, B. M.; Fleming, I., Eds.; Pergamon Press: New York, 1991; Vol. 8, p 667.

(7) Pyramidal inversion at phosphorus cannot be ruled out even though it was established that typically tertiary phosphines are configurationally stable at room temperature. See, for example: Gallagher, M. J.; Jenkins, I. D. In *Topics in Stereochemistry*; Eliel, E. L., Allinger, N. L., Eds.; Interscience Publishers: New York, 1968; Vol. 3, Chapter 1.

(8) Lauher, J. W.; Hoffmann, R. *J. Am. Chem. Soc.* **1976**, *98*, 1729.

(9) Albrand, J. P.; Gagnaire, D.; Picard, M.; Robert, J. B. *Tetrahedron Lett.* **1970**, 4593 and references therein.

(10) Quin, L. D.; Hughes, A. N. In *The Chemistry of Organophosphorus Compounds*; Patai, P., Series Ed.; Hartley, F. R., Ed.; John Wiley & Sons: New York, 1990; Vol. 1, Chapter 10.

(11) See, for example: (a) Awerbouch, O.; Kashman, Y. *Tetrahedron* **1975**, *31*, 33. (b) Moedritzer, K. Z. *Anorg. Allg. Chem.* **1979**, *458*, 183.

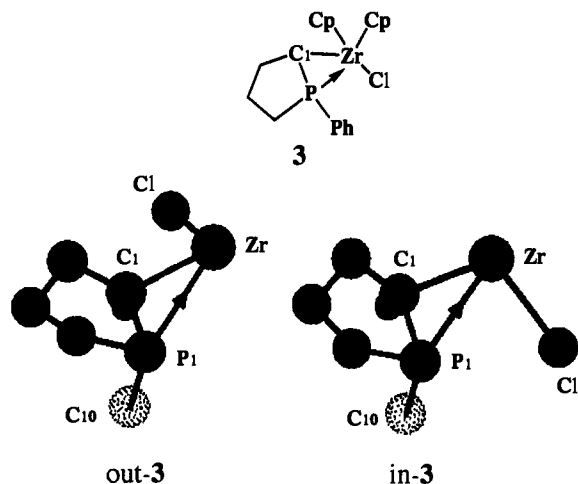
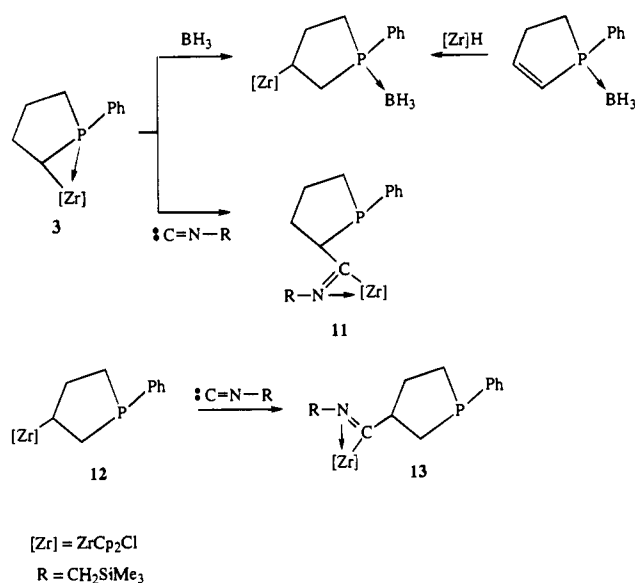


Figure 3. Molecular modeling of “in” and “out” structures of compound **3**. Cp groups on zirconium and hydrogen on endocyclic carbon atoms are omitted for clarity. The phenyl group linked to phosphorus is only represented by the ipso carbon C(10).

Scheme 4. Chemical Evidences for C–P–Zr Skeleton in **3**



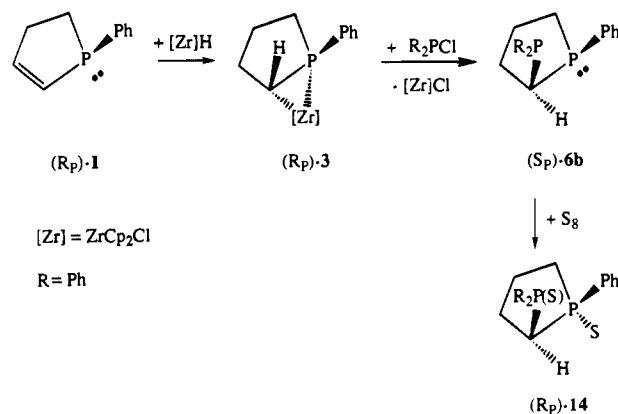
As it has been already well exemplified in the literature, the zirconium fragment in **11** was involved in a N–Zr dative bond.¹⁶ A small coupling constant ¹J_{CP} of 20.5 Hz characteristic for P(III)-phospholane¹⁹ confirmed further the structure of **11**, which was also corroborated by other NMR spectral data and mass spectrometry. It should be noted that this insertion of isocyanide into the C–Zr bond did not induce migration of the –C(=N–R)–ZrCp₂Cl fragment from the α to β position in the phospholane ring: this migration would give rise to compound **13**. No trace of **13** was detected. This latter product was available for comparison from reaction of the β-zirconated phospholane **12**, obtained from hydrozirconation of dihydrophosphole C₆H₅–P–CH₂–CH=CH–CH₂,⁵ with the corresponding isocyanide (Scheme 4).

With the well-established structure of **3** in hand it was further necessary to consider carefully the stereochemical stability at phosphorus in the phospholane compounds during the course

(19) ¹J_{CP} values in five-membered heterocyclic phosphines are in the range 14–26 Hz; ¹J_{CP} > 40 Hz for tetracoordinated phosphorus atom P(IV) of five-membered heterocycles.^{8,10,18}

(20) Cenac, N.; Zablocka, M.; Igau, A.; Majoral, J. P.; Pietrusiewicz, K. M. To be published.

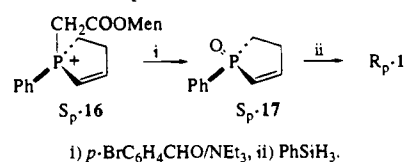
Scheme 5. Synthesis of the Optically Active Diphosphine (*S_P*)-**6b** and Diphosphine Disulfide (*R_P*)-**14**



of synthesis of diphosphines. For this purpose we have prepared the optically active dihydrophosphole (*R_P*)-**1**.²¹ This optically active dihydrophosphole (*R_P*)-**1** was reacted with [Cp₂ZrHCl]_n (**2**), giving rise to the expected α-zirconated phospholane **3***. Addition of Ph₂PCl to **3*** afforded the 1,1-diphosphine **6b***. This product was isolated in the form of the optically active diphosphine disulfide (*R_P*)-**14** ([α]_D²⁰ = –45.2) obtained in situ by the addition of sulfur to **6b*** (Scheme 5). The structure of (*R_P*)-**14** was confirmed by X-ray crystallography (Table 1). The ORTEP drawing of this derivative shows the atomic numbering scheme we have used in Figure 4. Selected bond lengths and angles are listed in Table 3. Cis arrangement was confirmed by the value of the C(10)–P(1)–C(1)–P(2) torsional angle: 5.1(2)°. As it is well documented, addition of sulfur on phosphine occurred with complete retention of configuration,²² Therefore it can be concluded that the absolute configuration at the phosphorus atom of the phospholane **6b** is (*S_P*). Consequently synthesis of (*S_P*)-**6b** from (*R_P*)-**1** (Scheme 5) occurred with retention of configuration at the intracyclic phosphorus atom. Indeed an *unprecedented* inversion of configuration at carbon took place during the exchange reaction between the α-zirconated phospholane **3** and chlorophosphines **4a,b** or phosphonium salts **5a,b**.²³

Synthesis of the bicyclic diphosphine **6c** prepared as the others by the procedure outlined in Scheme 1 brings a counter example. Chlorodiazaphospholane **4c** was treated with a THF solution of **3** at –20 °C; addition of sulfur to the resulting 1,1-diphosphine **6c** gave the corresponding dithio derivative **15**. NMR spectral data and mass spectrometry corroborated the diphosphine and diphosphine disulfide structures **6c** and **15**. Nevertheless the large coupling constant ²J_{PP} = 158.7 Hz observed for **6c** was in marked contrast with the values found for the other diphosphines (**6a**, ²J_{PP} = 37.5 Hz; **6b**, ²J_{PP} = 31.5 Hz; **6d**, ²J_{PP} = 40.1 Hz; **6e**, ²J_{PP} = 33.7 Hz). As ²J_{HP} values

(21) The phosphonium salt (*S_P*)-**16** was converted first into the corresponding phospholene oxide (*S_P*)-**17**. Reduction with PhSiH₃ gave (*R_P*)-**1**. Pietrusiewicz, K. M. To be published.



(22) See, for example: (a) Young, D. P.; McEwen, W. E.; Velez, D. C.; Johnson, J. W.; Van der Werf, C. A. *Tetrahedron Lett.* **1964**, 359. (b) Horner, L.; Winkler, H. *Tetrahedron Lett.* **1964**, 175.

(23) A process involving both inversion of configuration at phosphorus in the hydrozirconation and in the transmetalation steps is highly unlikely, although it cannot not be entirely ruled out.

Table 1. Crystallographic Data for Compound (*R_p*)-**14**

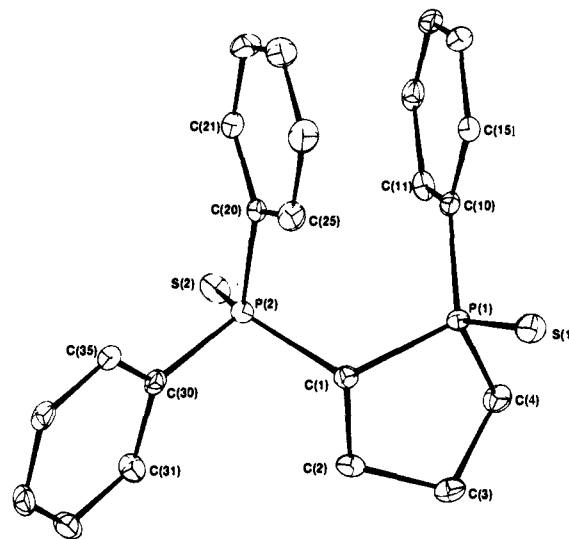
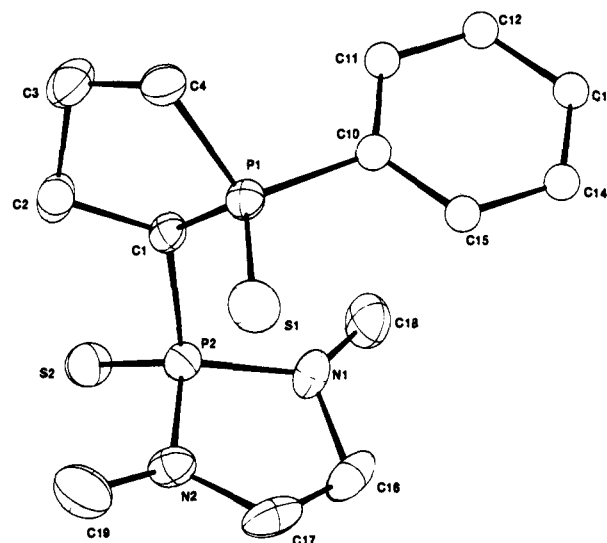
Crystal Parameters	
compd	C ₂₂ H ₂₂ P ₂ S ₂
fw (g)	412
cryst syst	orthorhombic
space group	<i>P</i> 2 ₁ 2 ₁
<i>a</i> , Å	8.391(5)
<i>b</i> , Å	10.880(3)
<i>c</i> , Å	22.651(6)
α	90
β	90
γ	90
<i>Z</i>	4
<i>V</i> , Å ³	2068(1)
ρ _{calcd} , g cm ⁻³	1.325
μ (Mo Kα), cm ⁻¹	4.03
cryst dims, mm	0.30 × 0.2 × 0.15
<i>T</i> , °C	-100
Data Collection	
diffractometer	Enraf Nonius CAD4F
monochromator	graphite
radiation	Mo Kα (λ = 0.71073)
scan type	ω/2θ
scan rate, deg/min	2.36–16.48
scan range θ, deg	0.8 + 0.345 tan θ
2θ range, deg	3 < 2θ < 50
no. of refln collected	3941 (± <i>h, k, l</i>)
no. of refln merged (<i>R_m</i>) (no Friedel)	3629 (0.054)
no. of refln used (<i>I</i> > 3σ(<i>I</i>))	3051
Refinement	
<i>R</i>	0.038
<i>R_w</i>	0.045
Flack parameter	0.05(10)
weighting scheme ^a	{ <i>w</i> = <i>w</i> '[1 - (Δ <i>F</i>)/6σ(<i>F_c)²]}²</i>
coeff Ar	4.80, -0.568, 3.12
goodness of fit	1.12
no. of params varied	237

^a *w*' = 1/Σ_{*r*=1,3} ArTr(*x*), where Ar are the coefficients for the Chebyshev polynomial Tr(*x*) with *x* = *F_c*/*F_c*(max).³¹

Table 2. Crystallographic Data for Compound **15**

Crystal Parameters	
formula	C ₁₄ H ₂₂ N ₂ P ₂ S ₂
formula wt	344.4
cryst syst	monoclinic
space group	<i>P</i> 2 ₁ / <i>C</i>
<i>Z</i>	4
<i>a</i> , Å	8.243(1)
<i>b</i> , Å	23.468(2)
<i>c</i> , Å	9.412(1)
β, deg	109.16(2)
<i>V</i> , Å ³	1719.9(6)
ρ _{calcd} , g cm ⁻³	1.330
cryst dims, mm	0.45 × 0.30 × 0.15
<i>T</i> , °C	20
Measurement of Intensity Data	
radiation (monochrome)	Mo Kα, 0.71073
scan type	ω/2θ
scan rate, deg/min	1.18–8.24
2θ range, deg	3 < 2θ < 50
no. of data collid	3020
no. of unique data (<i>F</i> ² > 3σ(<i>F</i> ²))	1865
no. of params varied	139
μ, cm ⁻¹	4.70
<i>R</i> (<i>F</i> ₀)	0.042
<i>R_w</i> (<i>F</i> ₀)	0.042
goodness of fit	1.18

(see above), ²*J*_{PP} values might be used in a first approach as a tool for deducing stereostructures: since R₂P groups were found in a pseudo-axial position in compounds **6a,b,d,e**, the diazaphospholane substituent should be in a pseudo-equatorial position in **6c**. X-ray structure determination of **15** confirmed

**Figure 4.** ORTEP drawing of the optically active diphosphine disulfide (*R_p*)-**14**. For clarity, hydrogen atoms are not represented.**Figure 5.** ORTEP drawing of the diphosphine disulfide **15**. For clarity, hydrogen atoms are not represented.**Table 3.** Selected Bond Distances (Å) and Angles (deg) for (*R_p*)-**14**

Distances			
P(1)–C(1)	1.869(4)	P(2)–C(1)	1.839(4)
P(1)–C(4)	1.809(4)	P(2)–C(20)	1.813(4)
P(1)–C(10)	1.800(4)	P(2)–C(30)	1.812(4)
P(1)–S(1)	1.955(1)	P(2)–S(2)	1.948(1)
Angles			
P(1)–C(1)–P(2)			119.4(2)
C(1)–P(1)–C(4)			95.1(2)
C(1)–P(1)–C(10)			112.6(2)
C(4)–P(1)–C(10)			111.0(2)
Torsion Angles			
C(10)–P(1)–C(1)–P(2)			5.1
C(10)–P(1)–C(1)–H(11)			124.9
C(10)–P(1)–C(1)–C(2)			122.2

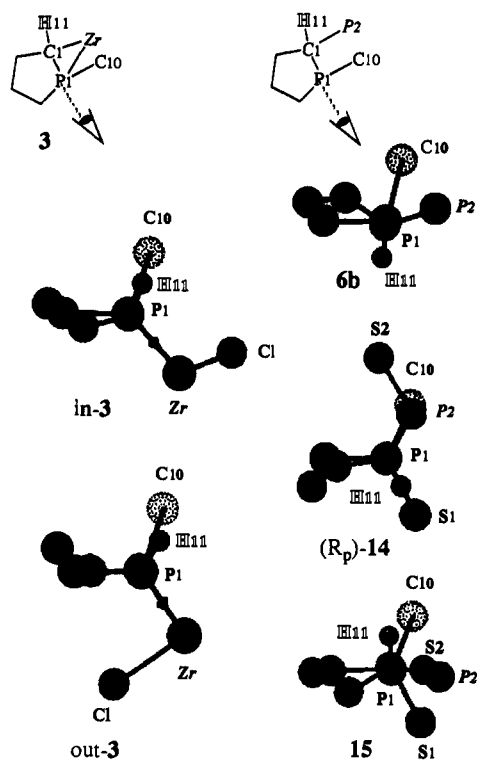
that the proton attached to C1 and the phenyl group on phosphorus P1 were cis (C(10)–P(1)–C(1)–H(11) torsion angle: 22.3 (5)°, see Tables 2, 4, and 5). Molecular modeling structures of **3** and X-ray data for **6b**, (*R_p*)-**14**, and **15** (Figure 6) clearly showed that, if inversion of configuration occurred when (*R_p*)-**14** and **15** were formed, such a process was not observed in the case of the synthesis of **15**.

Table 4. Selected Bond Distances (Å) and Angles (deg) for **15**

Distances			
P(1)–C(1)	1.836(4)	P(2)–C(1)	1.829(5)
P(1)–C(4)	1.818(6)	P(2)–N(1)	1.649(4)
P(1)–C(10)	1.802(3)	P(2)–N(2)	1.645(4)
P(1)–S(1)	1.952(2)	P(2)–S(2)	1.945(2)
Angles			
P(1)–C(1)–P(2)			120.5(2)
C(1)–P(1)–C(4)			93.3(2)
C(1)–P(1)–C(10)			106.5(2)
C(4)–P(1)–C(10)			110.1(2)
Torsion Angles			
C(10)–P(1)–C(1)–P(2)			82.0(3)
C(10)–P(1)–C(1)–H(11)			22.3(5)
C(10)–P(1)–C(1)–C(2)			143.3(3)

Table 5. Torsion Angle Values (deg) for in-**3**, out-**3**, **6b**, (*R_p*)-**14**, and **15** α -Substituted Phospholane Derivatives

	C(10)–P(1)–C(1)–Zr	C(10)–P(1)–C(1)–H(11)
in- 3	126.5	2.9
out- 3	118.3	14.9
	C(10)–P(1)–C(1)–P(2)	C(10)–P(1)–C(1)–H(11)
6b	56.0	170.0
(<i>R_p</i>)- 14	5.1	124.9
15	82.0	22.3

**Figure 6.** Views along P₁–C₁ axis: molecular modeling of compound **3** (“in” and “out” structures) and X-ray crystal structures of **6b**, (*R_p*)-**14**, and **15**. C₁₀ and H₁₁ proton were *cis* in **3** and *trans* in **6b** and **14**. Torsion angle values are listed in Table 5.

In conclusion, strong evidence for inversion of configuration at carbon during the electrophilic cleavage of the C–Zr bond of the α -zirconated phospholane **3** was found for the first time. This observation does not support the hypothesis of a four-membered transition state shown in Scheme 1.⁴ Some previous reports²⁴ described conditions for electrophilic cleavage of main group organometallics (and in some way, the d⁰ zirconium

system might well be modeled by main group species). It has been shown that the closed transition state was favored when an acceptor orbital was available on the metal (valence or hypervalent) and under conditions whereby solvation of an incipient cationic metallic residue, which would have been formed through an “open transition state” with inversion at carbon, was not feasible. They also showed that such open transition states were favored, with concomitant cleavage of the carbon–metal bond *with inversion of configuration* when stabilization of the incipient cationic metallic residue could occur, for example, by solvation. Thus, the stereochemistry of cleavage depends on the availability of a vacant orbital on the metal, *inter alia*. Others have also indicated the importance of steric effects in determining the stereochemical course of electrophilic cleavage of tin compounds. In most “classic” cleavage reactions of C–Zr, the zirconium is a “standard”, 16-electron, coordinatively unsaturated entity. Thus, a closed transition state is feasible. In our case, **3** is coordinatively saturated. Thus, with a strong phosphorus–zirconium interaction, the closed transition state would *not* be possible. In addition, with the strong interaction shown in Figure 3, the formation of a cationic zirconium, resulting from electrophilic cleavage with inversion at carbon, is stabilized.

However, in one case (formation of **6c**), the classical retention of configuration was observed. No satisfactory explanation (strength of the electrophile, steric hindrance, ...) of such a phenomenon can be given at present. Further investigations are underway involving kinetic studies with a large variety of electrophilic reagents in order to try to explain these discrepancies and to provide a complete mechanistic picture of this useful C–Zr cleavage reaction.

Experimental Section

General Procedure. All manipulations were performed under an argon atmosphere, either on a high-vacuum line using standard Schlenk techniques or in a Braun MB 200-G drybox. Solvents were freshly distilled from dark purple solutions of sodium/benzophenone ketyl (THF, toluene, benzene, diethyl ether), lithium aluminum hydride (pentane, *n*-hexanes), or CaH₂ (CH₂Cl₂, CHCl₃). C₆D₆ and THF-*d*₈ were treated with LiAlH₄, distilled, and stored under argon. Cp₂ZrCl₂ and :C=N–CH₂SiMe₃ were purchased from Aldrich and used without further purification. [Cp₂ZrHCl]_n (Schwartz’s reagent) (**2**) was synthesized by the method of Buchwald and co-workers.²⁵

Nuclear magnetic resonance (NMR) spectra were recorded at 25 °C on Bruker MSL 400, WM-250, and AC-200, and AC-80 Fourier transform spectrometers. The ¹³C NMR assignments were confirmed by proton-decoupled and/or selective heteronuclear-decoupled spectra. Positive chemical shifts are downfield given relative to Me₄Si (¹H, ¹³C) or H₃PO₄ (³¹P) references, respectively. Chemical analyses were performed by the analytical service of the Laboratoire de Chimie de Coordination (LCC) of the CNRS.

Preparation of 6c. To a magnetically stirred solution of **1**²⁶ (0.146 g, 0.9 mmol) in THF (5 mL) cooled at –20 °C was added a suspension of [Cp₂ZrHCl]_n (**2**) (0.232 g, 0.9 mmol) in THF (5 mL). The reaction mixture was stirred for 15 min at –20 °C then allowed to warm up slowly at room temperature and stirred for a further 3 h to give a dark brown homogeneous solution of **3**. The solution was cooled at –20 °C and chlorophosphine **4c** (0.146 g, 0.9 mmol) in CH₂Cl₂ (3 mL) was added via syringe. The reaction mixture was kept at –20 °C for 30 min then warmed up slowly to room temperature. The resulting colorless solution was evaporated to dryness. Successive extractions of the residue with pentane (2 × 20 mL) and diethyl ether (2 × 10 mL) gave the diphosphine **6c** as a white powder in 85% isolated yield. Anal. Calcd for C₁₄H₂₂N₂P₂: C, 59.83; H, 7.89. Found: C, 59.21; H, 8.02. ³¹P{¹H} NMR (C₆D₆): δ –15.4 (d, ²J_{PP} = 158.6 Hz, PPh), 123.7 (d, ²J_{PP} = 158.6 Hz, PN). ¹H NMR (C₆D₆): δ 1.50 (m, 2H, CH₂),

(25) Buchwald, S. L.; LaMaire, S. J. *Tetrahedron Lett.* **1987**, 28, 295.(26) Quin, L. D.; Mathewes, D. A. *J. Org. Chem.* **1964**, 29, 836.(24) Fukuto, J. M.; Jensen, F. R. *Acc. Chem. Res.* **1983**, 16, 177–184.

1.87 (m, 2H, CH₂), 2.50 (m, 5H, PCH and NCH₂), 2.56 (d, ³J_{HP} = 13.5 Hz, 3H, CH₃), 2.85 (d, ³J_{HP} = 13.5 Hz, 3H, CH₃), 2.99 (m, 2H, PCH₂), 7.14 (m, 3H, Ph), 7.48 (m, 2H, Ph). ¹³C{¹H} NMR (C₆D₆): δ 27.3 (dd, ²J_{CP} = 14.6 Hz, ²J_{CP} = 3.3 Hz, PhPCHCH₂), 29.6 (s, PhPCH₂CH₂), 31.1 (d, ¹J_{CP} = 23.6 Hz, PCH₂), 38.6 (d, ²J_{CP} = 20.9 Hz, NCH₃), 40.4 (dd, ²J_{CP} = 25.9 Hz, ³J_{CP} = 5.5 Hz, NCH₃), 47.6 (dd, ¹J_{CP} = 35.5 Hz, ¹J_{CP} = 23.2 Hz, CH), 54.6 (d, ²J_{CP} = 9.0 Hz, PNCH₂), 55.1 (d, ²J_{CP} = 7.6 Hz, PNCH₂), 127.7 (s, *p*-Ph), 128.3 (s, *m*-Ph), 131.3 (d, ²J_{CP} = 15.2 Hz, *o*-Ph), 136.2 (d, ¹J_{CP} = 19.8 Hz, *i*-Ph).

Preparation of 11. A THF solution (15 mL) of **3** (0.378 g, 0.9 mmol) and :C=N-CH₂SiMe₃ (0.127 mL, 0.9 mmol) was stirred at room temperature for 30 min. Volatiles were removed in vacuo. The residue was washed with pentane (3 × 7.5 mL), yielding 0.414 g of a white powder **11** (77% isolated yield). Anal. Calcd for C₂₅H₃₃ClNPSiZr: C, 56.31; H, 6.24. Found: C, 56.05; H, 6.28. ³¹P{¹H} NMR (THF): δ 0.7. ¹H NMR (THF-*d*₈): δ -0.04 (s, 9H, SiMe₃), 1.75–2.62 (m, 9H, CH and CH₂), 5.86, 5.95 (s, 10H, Cp), 7.31–7.47, 7.59–7.68 (m, 5H, Ph). ¹³C{¹H} NMR (THF-*d*₈): δ 1.04 (s, SiMe₃), 29.8 (d, ¹J_{CP} = 14.8 Hz, PCH₂), 30.2 (d, ²J_{CP} = 3.6 Hz, PCH₂CH₂), 36.5 (s, PCHZrCH₂), 43.1 (s, CH₂Si), 51.6 (d, ²J_{CP} = 20.5 Hz, PCHZr), 112.0 (s, Cp), 130.2 (s, *p*-Ph), 130.0 (d, ³J_{CP} = 6.8 Hz, *m*-Ph), 133.6 (d, ²J_{CP} = 19.3 Hz, *o*-Ph), 142.2 (d, ¹J_{CP} = 26.3 Hz, *i*-Ph), 235.5 (d, ²J_{CP} = 16.6 Hz, C=N).

Preparation of 13. In a procedure analogous to that given for **11**, treatment of **12** (0.378 g, 0.9 mmol) with :C=N-CH₂SiMe₃ (0.127 mL, 0.9 mmol) gave **13** (0.331 g, 62% isolated yield) as a white powder. Anal. Calcd for C₂₅H₃₃ClNPSiZr: C, 56.31; H, 6.24. Found: C, 56.12; H, 6.18. ³¹P{¹H} NMR (THF): δ -13.1. ¹H NMR (THF-*d*₈): δ 0.15 (s, 9H, SiMe₃), 2.17–2.67 (m, 9H, CH and CH₂), 5.98, 6.01 (s, 10H, Cp), 7.41–7.55, 7.61–7.69 (m, 5H, Ph). ¹³C{¹H} NMR (THF-*d*₈): δ 1.0 (s, SiMe₃), 28.7 (d, ¹J_{CP} = 16.2 Hz, PCH₂CH₂), 35.3 (d, ²J_{CP} = 3.6 Hz, PCH₂CH₂), 37.4 (d, ¹J_{CP} = 15.8 Hz, PCH₂CHZr), 43.7 (s, CH₂Si), 49.4 (d, ²J_{CP} = 3.8 Hz, PCH₂CHZr), 112.0 (s, Cp), 130.6 (s, *p*-Ph), 131.3 (d, ³J_{CP} = 3.9 Hz, *m*-Ph), 133.3 (d, ²J_{CP} = 15.3 Hz, *o*-Ph), 145.2 (d, ¹J_{CP} = 25.6 Hz, *i*-Ph), 237.2 (d, ³J_{CP} = 4.2 Hz, C=N).

Preparation of (R_P)-14. A Schlenk flask was charged with (R_P)-**1**²⁰ (0.163 g, 1.0 mmol), THF (5 mL), and a stir bar and cooled to -20 °C. Then a suspension of [Cp₂ZrHCl]₂ (**2**) (0.258 g, 1.0 mmol) in THF (5 mL) was added to the solution. The mixture was stirred for 15 min at -20 °C and allowed to warm slowly at room temperature and stirred for a further 3 h to give a dark brown homogeneous solution of (R_P)-**3**. The solution was cooled at -20 °C, and chlorophosphine **4b** (0.221 g, 1.0 mmol) in CH₂Cl₂ (3 mL) was added via syringe. The reaction mixture was kept at -20 °C for 30 min then warmed slowly to room temperature. The resulting colorless solution was evaporated to dryness. Extractions of the residue with pentane (2 × 20 mL) gave the diphosphine (S_P)-**6b** as a white powder. Addition of S₈ (0.128 g, 4.0 mmol) in a THF solution (10 mL) of (S_P)-**6b** gave (R_P)-**14**, which was isolated after column chromatography on silica gel 60 (70–230 mesh ASTM) using hexanes–diethyl ether (3:2) as an eluent (R_f = 0.32, 95% pure). The product was recrystallized from pentane–diethyl ether (1:1) to produce colorless crystals (0.310 g, 75% yield). Mp 142.5–143.0 °C. Anal. Calcd for C₂₂H₂₂P₂S₂: C, 63.94; H, 5.36. Found: C, 63.78; H, 5.45. ³¹P{¹H} NMR (C₆D₆): δ 43.4 (d, ²J_{PP} = 3.3 Hz, PPh), 61.8 (d, ²J_{PP} = 3.3 Hz, PPh₂). ¹H NMR (C₆D₆): δ 1.93 (m, 2H, CH₂), 2.15 (m, 2H, CH₂), 2.56 (m, 2H, CH₂), 3.81 (m, 1H, CH), 6.83–7.07 (m, 9H, Ph), 7.71–7.98 (m, 6H, Ph). ¹³C{¹H} NMR (C₆D₆): δ 24.5 (d, ²J_{CP} = 11.2 Hz, ²J_{CP} = 3.9 Hz, PhPCHCH₂), 29.6 (d, ²J_{CP} = 7.8 Hz, PhPCH₂CH₂), 35.8 (d, ¹J_{CP} = 56.7 Hz, PCH₂), 49.3 (dd, ¹J_{CP} = 45.0 Hz, ¹J_{CP} = 39.7 Hz, PCH), 127.1 (d, ³J_{CP} = 13.0 Hz, *m*-Ph), 130.7 (d, ²J_{CP} = 10.0 Hz, *o*-Ph), 130.9 (s, *p*-Ph), 131.4 (s, *p*-Ph₂), 132.2 (d, ³J_{CP} = 10.7 Hz, *m*-Ph₂), 134.1 (d, ²J_{CP} = 11.6 Hz, *o*-Ph).

Preparation of 15. A THF solution (10 mL) of **6c** (0.281 g, 1.0 mmol) and S₈ (0.128 g, 4.0 mmol) was stirred at room temperature for 3 h. Volatiles were removed in vacuo. Column chromatography of the residue on silica gel 60 (70–230 mesh ASTM) using CH₂Cl₂ as an eluent gave **15** (R_f = 0.42), which was recrystallized from benzene to produce colorless crystals (0.311 g, 95% isolated yield). Mp 164.5–165.0 °C. Anal. Calcd for C₁₄H₂₂N₂P₂S₂: C, 48.71; H, 6.42. Found: C, 48.59; H, 6.36. ³¹P{¹H} NMR (C₆D₆): δ 50.6 (d, ²J_{PP} = 7.0 Hz, PPh), 78.9 (d, ²J_{PP} = 7.0 Hz, PN). ¹H NMR (C₆D₆): δ 1.76 (m, 2H, CH₂), 1.86 (d, ³J_{HP} = 12.5 Hz, 3H, CH₃), 2.01 (m, 2H, CH₂), 2.29 (m,

2H, CH₂), 2.51 (m, 2H, NCH₂), 2.69 (d, ³J_{HP} = 10.5 Hz, 3H, CH₃), 2.77 (m, 2H, NCH₂), 2.99 (m, 2H, PCH₂), 7.03–7.06 (m, 3H, Ph), 7.58–7.67 (m, 2H, Ph), HCP obscured by CH₂ resonances. ¹³C{¹H} NMR (C₆D₆): δ 24.2 (d, ²J_{CP} = 14.6 Hz, PhPCHCH₂), 29.6 (d, ²J_{CP} = 13.1 Hz, PhPCH₂CH₂), 32.1 (d, ²J_{CP} = 3.2 Hz, NCH₃), 32.9 (d, ²J_{CP} = 7.7 Hz, NCH₃), 38.0 (d, ¹J_{CP} = 55.1 Hz, PCH₂), 48.7 (d, ²J_{CP} = 7.1 Hz, PNCH₂), 48.9 (d, ²J_{CP} = 8.4 Hz, PNCH₂), 55.3 (dd, ¹J_{CP} = 87.4 Hz, ¹J_{CP} = 42.1 Hz, CH), 127.7 (s, *p*-Ph), 128.3 (s, *m*-Ph), 131.3 (d, ²J_{CP} = 15.2 Hz, *o*-Ph), 136.2 (d, ¹J_{CP} = 19.8 Hz, *i*-Ph).

X-ray Crystallographic Analyses for (R_P)-14. A selected crystal was mounted on an automatic diffractometer CAD4-F. Unit cell dimensions with estimated standard deviations were obtained from least-squares refinements of the setting of 25 well-centered reflections. Three standard reflections were monitored periodically; they showed no change during data collections carried out at low temperature (-100 °C). Crystallographic data and other pertinent information are summarized in Table 1. Corrections were made for Lorentz and polarization effects. Computations were performed by using the CRYSTALS program²⁷ adapted to a PC. Atomic form factors for neutral P, S, C, and H atoms were taken from ref 28; anomalous dispersion was taken into account for P and S atoms. The structure was solved by direct methods using the SHELX86 program.²⁹ The hydrogen atoms attached to the C atoms were located on difference Fourier, but their coordinates were introduced in refinement as fixed contributors in calculated positions and recalculated after each cycle. They were assigned isotropic thermal parameters 20% higher than those of the carbon to which they were attached. The absolute configuration was assigned on the basis of the refinement of the Flack's enantiomorph parameter, *x*,³⁰ which is the fractional contribution of *F*(-*h*) to the observed structure amplitude as depicted in the following formula:

$$F_o^2 = (1 - x)F(h)^2 + xF(-h)^2$$

It is sensitive to the polarity of the structure and was found to be close to 0, which clearly indicated the correctness of the original enantiomer choice. Anisotropic temperature factors were introduced for all non-hydrogen atoms. Full-matrix least-squares refinements were carried out by minimizing the function $\sum w(|F_o| - |F_c|)^2$, where *F*_o and *F*_c are the observed and calculated structure factors. Models reached convergence with

$$R = \frac{\sum (||F_o| - |F_c||)}{\sum |F_o|} \quad \text{and} \quad R_w = \left[\frac{\sum w(|F_o| - |F_c|)^2}{\sum w(F_o)^2} \right]^{1/2}$$

having values listed in Table 1. Criteria for a satisfactory complete analysis were the ratio of rms shift to standard deviation being less than 0.1 and no significant features in final difference maps.

X-ray Crystallographic Analyses for 15. The diffraction data for the compound C₁₄H₂₂N₂P₂S₂ were collected at low temperature (20 °C) on a four-circle ENRAF-NONIUS CAD4F diffractometer. Unit cell dimensions with estimated standard deviations were obtained from a least-squares fit of the setting angles of 25 reflections with 12.0 °C < θ < 14.5 °C. Reduction to *F*_o and σ(*F*_o), corrections for background, attenuator, and LP in the usual manner.²⁷ No significant standard variations (0.7%). All measured reflections unique. Empirical absorption corrections³² (*T*_{min} = 0.937, *T*_{max} = 0.998). More details on data collection and refinements are given in Table 2.

(27) Watkin, D. J.; Carruthers, J. R.; Betteridge, P. W. *CRYSTAL User Guide*; Chemical Crystallography Laboratory, University of Oxford: Oxford, U.K., 1985.

(28) *International Tables for X-ray Crystallography*; Kynoch Press: Birmingham, England, 1974; Vol IV.

(29) Sheldrick, G. M. *SHELXS 86, Program for Crystal Structure Solution*; University of Göttingen: Göttingen, Germany, 1986.

(30) Flack, H. *Acta Crystallogr.* **1983**, *A39*, 876–881.

(31) Prince, E. *Mathematical Techniques in Crystallography*; Springer-Verlag: Berlin, 1982.

(32) North, A. C. T.; Phillips, D. C.; Mathews, F. S. *Acta Crystallogr., Sect. A* **1968**, *A21*, 351–359.

The structure was solved by direct methods using the SHELXS86 program.²⁹ Full-matrix least-squares refinement using SHELX76,³³ All non-hydrogen atoms were anisotropically refined except those of the phenyl ring which were refined as an isotropic rigid group. Hydrogen atoms were located on difference Fourier map, introduced in calculations in a constrained geometry (C–H = 0.97 Å), with isotropic thermal parameters first refined, then kept fixed to 0.05 Å² for H(11) and to 0.07 Å² for other ones. Scattering factors (f' , f'') are taken from International Tables for X-ray Crystallography.

Acknowledgment. Financial support of this work by the CNRS, France, and by State Committee for Scientific Research, Poland (Grant No. 2.1307.91.01), is gratefully acknowledged.

(33) Sheldrick, G. M. *SHELXS 76, Program for Crystal Structure Determination*; University of Cambridge: Cambridge, England, 1976.

We also thank the NMR service of the LCC, Gérard Comenges, Francis Lacassin, and Gilles Pelletier for helpful assistance and discussions,

Supporting Information Available: Tables of crystallographic data, atomic coordinates, bond distances and angles, positional parameters, and anisotropic thermal parameters for (*R_p*)-**14** and **15** (12 pages); listing of structure factors for (*R_p*)-**14** and **15** (8 pages). This material is contained in many libraries on microfiche, immediately follows this article in the microfilm version of the journal, can be ordered from the ACS, and can be downloaded from the Internet; see any current masthead page for ordering information and Internet access instructions.

JA950014I